



Origin of temporal changes of inner-core seismic waves

Yi Yang ^a, Xiaodong Song ^{a,b,*}

^a Department of Geology, University of Illinois at Urbana-Champaign, Urbana, USA

^b Institute of Theoretical and Applied Geophysics, School of Earth and Space Sciences, Peking University, Beijing, China



ARTICLE INFO

Article history:

Received 7 February 2020

Received in revised form 19 March 2020

Accepted 4 April 2020

Available online 30 April 2020

Editor: M. Ishii

Keywords:

inner core rotation

waveform doublet

temporal change

PKIKP

PKIKP

ABSTRACT

Temporal changes of inner-core (IC) seismic phases have been confirmed with high-quality waveform doublets. However, the nature of the temporal changes is still controversial. We investigated systematically the temporal changes of IC refracted (PKIKP) and reflected (PKiKP) waves with a large data set of waveform doublets. We used non-IC reference phase (mainly SKP), which eliminated ambiguity where the temporal changes come from. We found that the temporal changes have always started at refracted PKIKP and the travel time changes correlate better with PKIKP. Changes in reflected PKiKP can be easily contaminated by the strong and time-varying PKIKP and coda wave trains and therefore are not reliable indicators for IC boundary changes. Combining with previous observations, we conclude that the temporal changes come mostly (if not all) from the IC interior and IC surface changes as the sole source suggested previously can be ruled out. The differential rotation of the IC shifting its heterogeneous uppermost structures is the simplest and most reasonable explanation for the origin of the time-varying IC waves. A rotation rate of about 0.05–0.1° per year with possible decadal fluctuation can reconcile all temporal change observations from body waves, IC scattering, and normal mode data.

© 2020 Elsevier B.V. All rights reserved.

1. Introduction

Temporal changes of the inner core (IC) on decadal time scale have been confirmed by many seismic body-wave observations, especially those from high-quality repeating earthquakes (e.g., Zhang et al., 2005). It was first discovered by Song and Richards (1996) from progressively earlier PKIKP (DF) arrivals traversing the IC (Fig. 1) mainly from events in South Sandwich Islands (SSI) region recorded by the College (COL) station in Alaska. The time-varying DF has generally been interpreted as the differential rotation of the IC with respect to the mantle shifting the laterally heterogeneous IC (e.g., Creager, 1997; Zhang et al., 2005). Subsequently, the PKiKP (CD) arrivals (Fig. 1) reflecting off the IC boundary (ICB) were also found to exhibit temporal changes over several years (Wen, 2006; Cao et al., 2007; Song and Dai, 2008; Xin et al., 2015; Yao et al., 2015), from SSI repeating earthquakes to stations in Central Asia and Canada, sampling two spots beneath Southern Africa and Central America, respectively. The time-varying CD suggests a very dynamic ICB with rapid localized crystallization from the liquid outer core or melting of the ICB (Wen, 2006; Yao et al., 2015; Yao et al., 2019), small-scale topography of the ICB shifted by the

differential rotation (Cao et al., 2007), or solidified iron patches in a mushy layer (Fearn et al., 1981) shifted by the outer core convection (Song and Dai, 2008).

Although the existence of IC temporal changes was challenged in the past (e.g., Souriau et al., 1997; Poupinet et al., 2000), it has been supported by many studies (Creager, 1997; Song, 2000; Vidale et al., 2000; Song, 2001; Tkalcic et al., 2013; Vidale, 2019). The debate was resolved in a joint study by both parties in favor of IC temporal changes and IC rotation (Sun et al., 2006) and the existence had been well accepted after the doublet study by Zhang et al. (2005). However, models for the IC temporal changes remain controversial. Estimates of the rotation rate vary orders of magnitude, from several degrees per million years (Waszek et al., 2011), marginally significant (0.13 with one standard deviation of 0.11 deg/yr) (Laske and Masters, 2003), a few hundredths (0.05–0.07) of deg/yr (Vidale, 2019; Yang and Song, 2020), to a few fractions of a deg/yr (by many studies, e.g., Creager, 1997; Zhang et al., 2005; Cao et al., 2007). Furthermore, the rotation model might be rejected (Mäkinen and Deuss, 2011; Yao et al., 2019). The recent study by Yao et al. (2019) is significant as they have considered the DF and CD as well as their coda waves and conclude that the temporal changes of the IC seismic phases are caused entirely by the temporal changes at the ICB.

In this study, we investigated the time-varying DF and CD arrivals using moderate-sized repeating earthquakes (also known as waveform doublets) (Poupinet et al., 1984). We used globally dis-

* Corresponding author at: Department of Geology, University of Illinois at Urbana-Champaign, Urbana, USA; now at Institute of Theoretical and Applied Geophysics, School of Earth and Space Sciences, Peking University, Beijing, China.

E-mail address: xiao.d.song@gmail.com (X. Song).

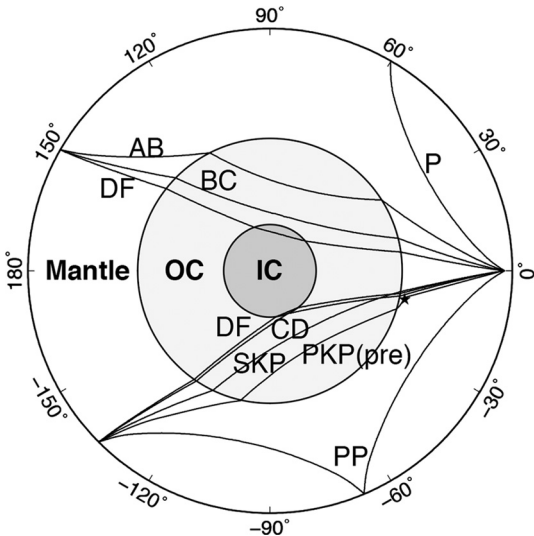


Fig. 1. Illustration of the ray paths of seismic phases used in this study. The example event at 0° and 200-km depth is recorded by 3 receivers at the distance of 60° , 135° and 150° , respectively. The phases include inner core phases PKP (DF, CD) and non-inner core phases PKP (BC, AB), P, PP, SKP, and PKP precursor (with scattering, star, in the lowermost mantle). Abbreviations: IC, inner core; OC, outer core; PKP(pre), PKP precursors.

tributed events as well as in the SSI region, which provided initial and strongest evidence for the temporal changes of the ICB (Wen, 2006; Cao et al., 2007; Song and Dai, 2008). Our new results show that temporal changes always start from the DF phase and that the previously reported temporal changes of CD are likely contaminated by time-varying DF wave trains. We laid out several lines of evidence that temporal changes from below the ICB are required and a differential rotation is still the best way to explain the IC temporal changes.

2. Data

We used two data sets of waveform doublets to examine the temporal changes of DF and CD arrivals at the distance range between 128° and 142° . One is a global data set of high-quality waveform doublets with magnitude at least 5.0 (Table S1). It is a subset of our recent systematic global search (Yang and Song, 2020), with clear target phases and time lapse of at least 6 years between the two events of the doublet imposed to ensure temporal changes could be observed if any (Song and Dai, 2008). The non-IC (including mantle and outer-core) phases (Fig. 1) of the doublets recorded by all available seismic stations should be nearly identical, with average cross-correlation coefficient (CC) at least 0.95 over a 15-s window. The total number of doublets is 39 using data from 1992 to 2017. The number of non-IC phases ranges from 8 to 197 with the median of 43. The doublet quality under such criteria is extremely high. For example, the 1993 and 2003 SSI doublet (ID 1993335_2003249 in Table S2 or simply referred as 9303 hereafter), which is among the best of previous studies (Zhang et al., 2005; Wen, 2006; Cao et al., 2007), has an average CC of only 0.919 with 9 non-IC phases.

Another data set is waveform doublets of slightly inferior quality in the SSI region (a total of 25 pairs, Table S2). We slightly lowered down the cut-off CC to 0.90 and cut-off magnitude to 4.7 to include some old pairs reported by previous studies and also many new pairs of similar quality. Like above, all pairs have time lapses of at least 6 years, except for a few old pairs from Song and Dai (2008) with lapses close to 6 years.

We used broadband high-gain vertical-component (BHZ) channels only, except some short-period (SHZ) data from the Yel-

lowknife array (YKA) in Canada from the SSI doublets, sampling the anomalous ICB beneath Central America. The array data from YKA were linearly stacked to enhance the signal-to-noise ratio (SNR). The procedure to stack the YKA data is the same for either event of the doublet to ensure consistency between the two events. In addition, the waveform data were preprocessed in a series of procedures as in Xin et al. (2015): (1) removing the mean and trend, (2) integrating from velocity to displacement records, (3) convolving with the WWSSN Short-Period (WWSP) response, and (4) bandpass filtering from 0.6 to 3.0 Hz.

3. Detecting temporal changes of the IC

The IC temporal changes can be revealed by differential arrival times and dissimilar waveforms of the IC arrivals and their coda waves from waveform doublets (Zhang et al., 2005). The arrival time difference (dt) of an IC phase between a pair comes mainly from origin time errors, clock errors of stations, tiny separation between the two sources, heterogeneity of tiny path difference, random noise errors, and temporal changes along the raypath. Relocations (e.g., Zhang et al., 2005; Wen, 2006) can largely remove the influence from earthquake locations, origin time errors, and obvious large clock errors (outliers of over a few fractions of a second). However, we recently found that small random clock errors of stations can be significant for studying the temporal changes (with standard deviation of 0.077 s) (Yang and Song, 2020), which are at the same order of or greater than the observed IC temporal changes. Previous studies by Wen (2006), Yao et al. (2015) and Yao et al. (2019) corrected for relocations but did not consider small random clock errors. Because the random clock errors in individual measurements cannot be removed from relocations, it needs to be extremely cautious to rely on absolute travel times to study temporal changes of the media.

In this study, we used non-IC phase as reference to eliminate clock errors before studying the temporal changes of the IC phases (Figs. 2–4, 6; Tables S3–S5). We formed double differential time (ddt) between two phases and between the two events of the doublet. The ddt between the arrival times $t(A)$ and $t(B)$ of phases A and B, respectively, from a doublet is defined as follows (Song and Dai, 2008), $ddt(A - B) = dt(A) - dt(B) = (t(A_2) - t(A_1)) - (t(B_2) - t(B_1))$, where the subscripts 1 and 2 denote the earlier and the later events of the doublet, respectively. All the original differential time measurements are listed in Tables S3–S5. Using ddt can largely eliminate the aforementioned errors, especially the origin time and clock errors, since the common errors in dt are canceled in the differentiation. For example, $ddt(BC-DF)$ and $ddt(CD-DF)$ can be used to detect the temporal variations of the IC (Li and Richards, 2003; Zhang et al., 2005; Song and Dai, 2008; Xin et al., 2015).

The non-IC SKP phase is often observable in the same seismogram as the PKP phases (DF and CD) at our distance range (128° and 142°), providing an excellent reference phase. We do need to consider the separation of the two events of the doublet, which are not exactly co-located. The separation is relatively tiny, usually within a few hundred meters horizontally and less than 1 km vertically for the inferior doublets (e.g., Zhang et al., 2005; Wen, 2006; Yang and Song, 2020). Using the horizontal separation of 370 meters for the 9303 doublet (Wen, 2006), the predicted $ddt(SKP-CD)$ and $ddt(SKP-DF)$ from the location difference is up to ~ 0.004 s for a 1-D reference model. The vertical separation has negligible effect. The location difference has negligible effect on $ddt(CD-DF)$ as their ray parameters are very similar. Thus, in this study, we didn't correct for the location difference. Influences from 3-D mantle heterogeneity of tiny path difference and from data noise are treated as small random errors, which we estimated to have a standard deviation of ~ 0.01 s (Yang and Song, 2020). We also used man-

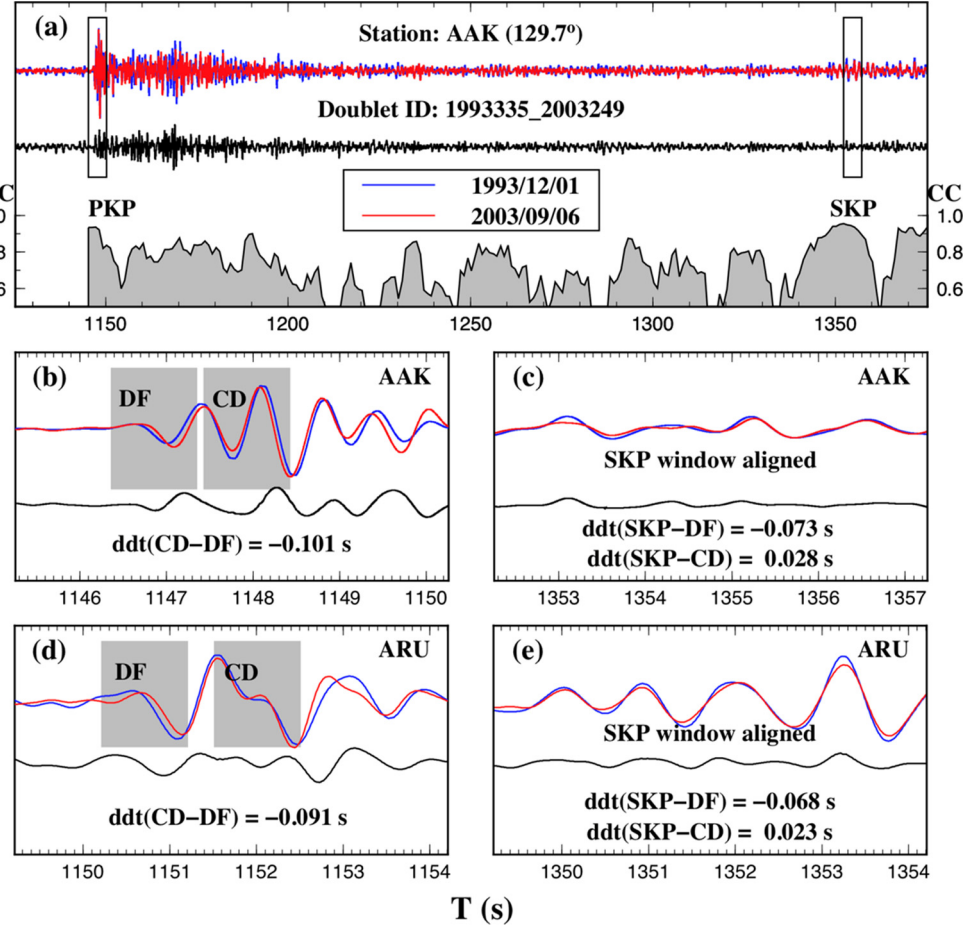


Fig. 2. Display of an example waveform doublet and IC temporal changes. The doublet (1993335_2003249), although still an inferior one in this study, is a very good and well-known pair used in previous studies (Zhang et al., 2005; Wen, 2006; Cao et al., 2007). The IC temporal changes at stations AAK (a, b, and c) and ARU (d, e) were first identified by Wen (2006). The gray area in (a) depicts the sliding cross-correlation coefficients (CC) using 5-s windows and 1-s steps starting right before PKP arrivals as shown in the box on the left of (a) and the enlarged view in (b). Note the CC starts from 0.5 to 1.0 to show better the high correlation in the vicinity of SKP. The waveform of the later event in 2003 (red) is shifted to align with that of the earlier event in 1993 (blue) at the SKP window (with the highest CC of 0.955 in the entire wave train) on the right of (a) and an enlarged view in (c). The black line in each panel is the differential waveform computed by subtracting the later one from the earlier one after aligning and normalizing the waveforms. The two shaded boxes in (b) represent the time window for measuring the time shift of DF and CD. The panels (d, e) are plotted in the same way as the panels (b, c). The DF waveforms at both AAK and ARU show clear time shifts after aligning with SKP. (For interpretation of the colors in the figure(s), the reader is referred to the web version of this article.)

tle phase PP as the reference phase for a few (9 in Table S5) SSI doublets to YKA. The quality of the PP phase is generally inferior to SKP, thus we used PP only when the CC of SKP is smaller than 0.85 and the CC of PP is greater than 0.85. The location difference has stronger effect on $ddt(PP-PKP)$. A horizontal separation of 370 meters would result in $ddt(PP-DF)$ of up to ~ 0.012 s for a 1-D reference model. We didn't correct for the location difference either when aligning with the PP phase. There are only a few doublets using the PP reference (Fig. 3, Table S5), which are not used for the subsequent ddt analyses. Correcting for the location wouldn't make a difference in the waveform display (Fig. 3).

The dt for each phase is computed by cross-correlation in time domain. The length of time windows is ~ 1 s containing the phase for the two IC phases, as they are separated only by 1-3 s. The time window for SKP or PP is 5 s and is automatically searched out using sliding cross-correlation (e.g., Fig. 2) to find the most coherent and generally most energetic 5-s window near the predicted time of SKP or PP relative to DF (hand-picked) by IASP91 model (Kennett and Engdahl, 1991) and the catalog location of the earlier event. In addition, we resampled the waveforms to 0.001 s intervals (originally at the sampling rate of 0.025 or 0.050 s) to improve the precision of dt and ddt measurements. Influence on the time shift from background noise is not considered here, as we

only used high-quality waveforms with SNR of DF or CD (peak energy divided by the RMS of 10 s preceding noise) of at least 10.0 for both events of the doublets. The dissimilarity of waveform is often indicated by relatively low CC and can be easily identified by manual inspection. We also computed the differential waveform by subtracting the waveform of the later event from that of the earlier event after normalization by their peak-trough amplitudes and alignment by the times of the SKP (or PP) phase.

4. Source of the temporal changes

We first examined the two prominent anomalous paths reported previously and then our large global data set.

4.1. Southern Africa anomaly

The time-varying CD beneath Southern Africa was first reported by Wen (2006) using the 9303 doublet, recorded by stations ARU, AAK, and OBN. The station OBN is at the distance around 123° so that the waveform of CD and DF arrive closely together within half wave cycle (~ 0.5 s), thus it is difficult to determine whether any temporal change is from the CD or DF phase. We re-examined the other two stations, AAK and ARU.

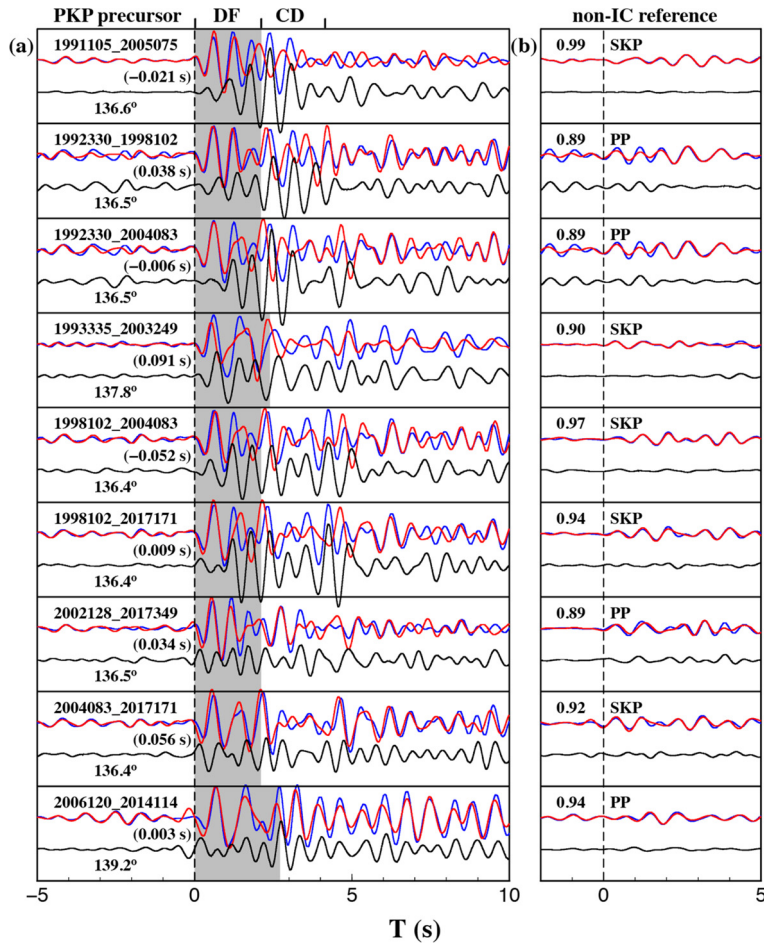


Fig. 3. Example waveform comparisons of SSI doublets recorded by Yellowknife array (YKA). In each window, the waveforms of the two events (blue, earlier event; red, later event) are aligned by the non-IC phase (SKP or PP, with CC labeled) and normalized by their peak-trough amplitudes and the black line is the differential waveform between the two traces. Note that the relative amplitude between (a) and (b) for the earlier event are reserved. The panel (a) shows the waveforms of PKP waves, coda, and precursors, while the panel (b) shows the waveforms of the non-IC phase. The arrival times of the DF in (a) and non-IC in (b) are set to 0. The relative time shifts of the first wave cycle of DF in (a), i.e. $ddt(\text{non-IC} - \text{DF})$, are marked in the parentheses near the onsets of DF phases (Table S5). The shaded areas in (a) represent the predicted time from DF to CD by the IASP91 model (Kennett and Engdahl, 1991).

After relocation, the alignment of DF is better than that of CD for both AAK and ARU stations, suggesting CD is anomalous (Wen, 2006). However, both stations have consistent SKP arrivals for both events of the doublet. When the waveforms are aligned with the SKP, they are obviously misaligned from the onset of DF for both stations (Fig. 2). The results suggest robust temporal changes from the refracted DF as well as obvious clock problems in the relocation. The $ddt(\text{SKP-DF})$ and $ddt(\text{SKP-CD})$ are -0.073 s and 0.028 s for AAK, respectively, and -0.068 s and 0.023 s for ARU, respectively. In addition, since the coda of DF is very energetic and time-varying as shown in Fig. 2, the changes in CD are likely contaminated by the DF coda. Consequently, we determined that temporal changes occur on DF arrivals, but temporal changes cannot be confirmed on the CD arrivals as originally determined from relocation (Wen, 2006). See more discussion on these two paths below.

4.2. Central America anomaly

Previous studies using a few pairs of waveform doublets from SSI to stacked YKA reported temporal changes under Central America in CD mostly, in terms of amplitude (Cao et al., 2007) and arrival times (Song and Dai, 2008), indicating time-varying ICB over several years. We used 23 pairs of SSI doublets with clear IC arrivals to reinvestigate this path (Table S5). All of our pairs also have clear and consistent stacked non-IC SKP or PP phase.

The waveforms of the IC arrivals recorded by YKA (stacked) are complex with energetic coda and sometimes observable PKP precursors (Fig. 3). The amplitudes of precursors are relatively weak so that the onsets of the DF arrivals are clear. However, the CD arrivals, following the DF windows (shaded) of ~ 2 s, are weak and buried in the wave trains and thus are difficult to identify. Assuming that the wave cycle at the predicted time by IASP91 model (Kennett and Engdahl, 1991) is mostly CD phase, we observed non-zero $ddt(\text{SKP-DF})$ up to 0.09 s but $ddt(\text{SKP-CD})$ as large as -0.29 s (Table S5). The magnitude of $ddt(\text{SKP-CD})$ is much larger than the $ddt(\text{SKP-DF})$, indicating CD would be much more anomalous than DF.

However, similar to the Southern Africa anomaly, the onset of temporal changes always starts from DF rather than CD, when the waveforms are aligned with SKP (or PP) (Fig. 3). The waveform changes are visible from the very beginning cycle of the DF and the differential waveforms display very large amplitudes, sometimes even comparable to the amplitudes of the original waveforms. Most importantly, the shaded areas after the DF onsets and before the predicted times of CD (relative to DF) always show very significant temporal changes of the waveforms. The waveform differences for several pairs (e.g., 1993335_2003249, 1998102_2004084, 2002128_2017349, 2004083_2017171) are larger in the shaded windows than in the subsequent windows. In contrast, pairs with precursors of sufficiently high SNRs (e.g., 1991105_2005075, one

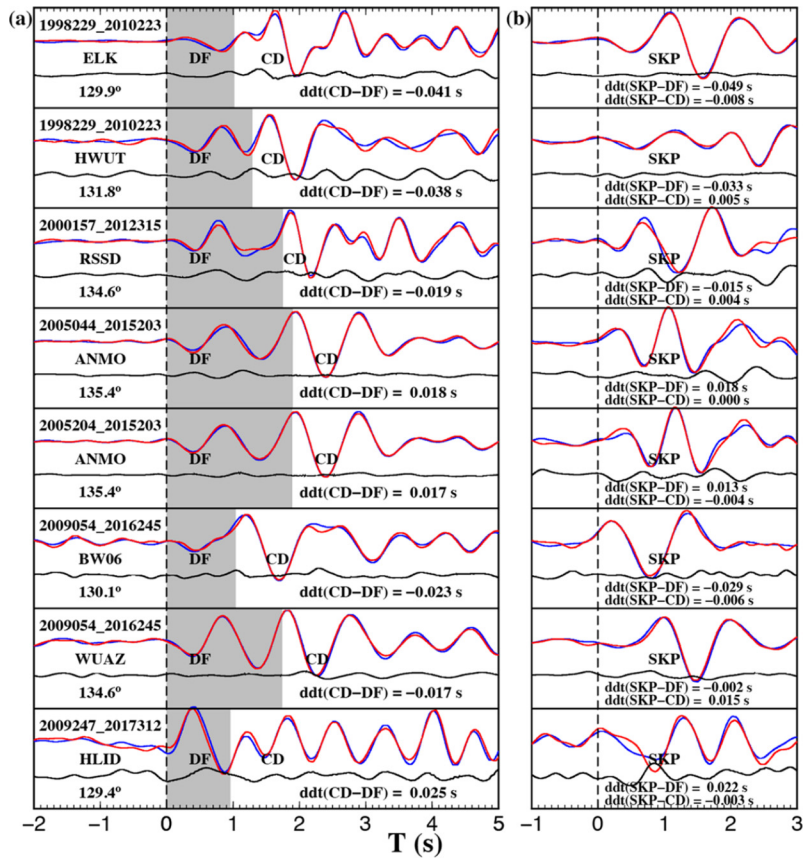


Fig. 4. Example high-quality doublets with relatively large IC temporal changes. The plot shows all the high-quality pairs with clear PKP (a) and SKP (b) and absolute $ddt(CD-DF)$ of at least 0.015 s. The waveforms and shaded areas are plotted similarly to those in Fig. 3. The doublet ID, station code, distance, and ddt measurements are labeled.

of the best-quality SSI pairs) also show little energy in the differential waveforms, providing yet another powerful reference to the dissimilarity of the DF and its coda energy (Fig. 3). Compared to other paths (e.g., Figs. 2 and 4), the waveforms of this path between the two events of the doublet are much less coherent after the onsets of the DF phase probably due to the time-varying DF waveforms and strong coda (Fig. 3). Such time-varying DF waveforms and energetic coda, at the distance of $\sim 150^\circ$ where CD is absent, are also observed along the SSI to Alaska path (Zhang et al., 2005; Yao et al., 2019), which is very close to the SSI to YKA path in the IC. The strong DF coda from SSI to YKA or Alaska sampling the IC beneath the Central America, despite strong IC attenuation (e.g., Cormier and Li, 2002), as well as the prominent changes of DF and coda waveforms are peculiar and could be related to highly heterogeneous IC structure of the region with strong anisotropy (Creager, 1992; Song and Helmberger, 1993; Song and Xu, 2002). The large DF waveform difference makes it difficult to discern how much energy of the temporal changes in the CD window is from the DF coda waves and how much is from the reflection off the ICB. However, the waveform difference from the very onset of the DF and in the subsequent coda make it certain that the DF energy would affect the later-arriving CD in travel times and in amplitudes for this path. The results suggest that the changes in the CD window are not reliable indicators for the ICB temporal changes, contrary to previous studies (Wen, 2006; Cao et al., 2007; Song and Dai, 2008).

4.3. A global view

We measured $ddt(CD-DF)$ from the high-quality global doublets (examples in Fig. 4) and slightly inferior SSI doublets (with time

separation of at least 6 years) (see Data session above). Fig. 5 shows a map of all the 107 $ddt(CD-DF)$ measurements (Table S3 and S4). Besides the Southern Africa and Central America areas, we found only one more spot beneath Japan and its vicinity with two relatively large $ddt(CD-DF)$ measurements (-0.041 and -0.038 s). The two measurements are from the same doublet in the Java trench recorded by two nearby stations in northwest US. They both have clear mantle SKP phase (top 2 panels of Fig. 4), with $ddt(SKP-DF)$ of -0.049 and -0.033 s and $ddt(SKP-CD)$ of only -0.008 and 0.005 s.

There are 41 paths with clear and consistent SKP arrivals with CC of SKP of at least 0.90 among all the paths in Fig. 5 (25 from the high-quality doublets and 16 from the slightly inferior SSI doublets). We measured the $ddt(SKP-DF)$ and $ddt(SKP-CD)$ for these paths and compared with $ddt(CD-DF)$ respectively (Fig. 6). Because of the strong DF coda and the mixing of DF and CD energy in the SSI-YKA paths (Fig. 3 and discussion above), these paths were not used in Fig. 6. We can see that the $ddt(SKP-DF)$ displays much better correlations with $ddt(CD-DF)$. The coefficients of determination (R^2 values) of the linear regressions (Fig. 6) are 0.713 and 0.715 for the best quality doublets and for the measurements when the slightly inferior doublets are also included, respectively; while the R^2 values between $ddt(SKP-CD)$ and $ddt(CD-DF)$ are only 0.061 and 0.141, respectively, for the two cases.

The linear regressions from the high-quality and slightly inferior doublets are similar, suggesting 81–86% of the $ddt(CD-DF)$ comes from the DF and 14–19% comes from the CD. The two largest observed $ddt(CD-DF)$ values are 0.101 and 0.091 s (9303 doublet to AAK and ARU, respectively; Fig. 3). The largest contributions from the CD would be less than 0.02 s from the above inferred percentage contribution. On the other hand, we estimated

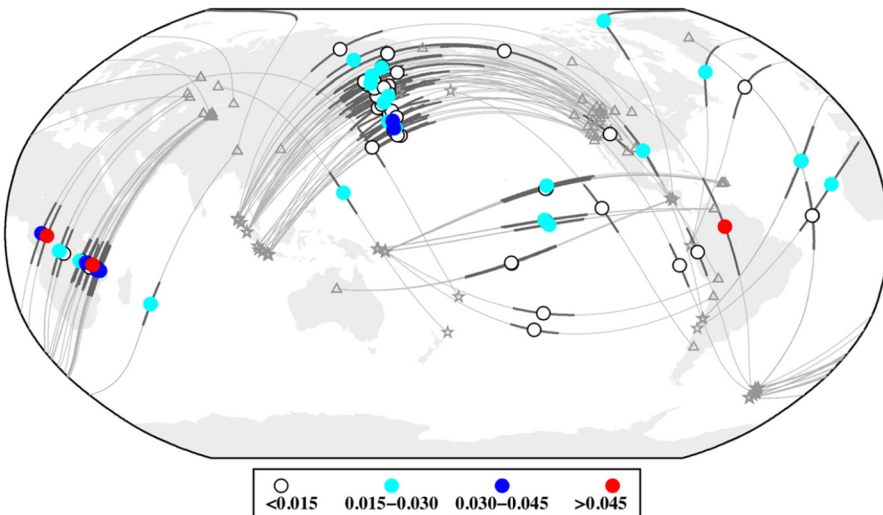


Fig. 5. Map of $ddt(CD-DF)$ measurements from both high-quality global doublets and slightly inferior SSI doublets. The gray lines are the surface projections of the raypaths from events (stars) to stations (triangles), with the inner-core segments in thickened dark gray lines. The absolute values of ddt measurements are plotted at the bottoming points of DF (circles) with the legend shown. Note that only one example of SSI to YKA paths (see Table S5) is plotted to avoid overcrowding.

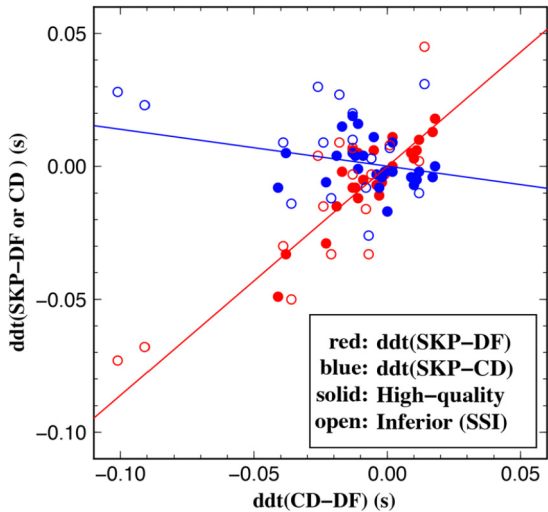


Fig. 6. The double differential time $ddt(CD-DF)$ versus $ddt(SKp-CD)$ (blue) or $ddt(SKp-DF)$ (red) from the high-quality (solid) and slightly inferior quality (open) doublets with clear and consistent SKP arrivals. The two colored lines show the linear regressions of the high-quality data (solid circles) of the corresponding colors. The slopes for the red and blue lines are 0.861 ± 0.114 and -0.139 ± 0.114 , respectively. The linear regressions for the inferior data set (open circles) are similar (not shown), which are 0.814 ± 0.141 and -0.186 ± 0.141 , respectively.

the standard deviations of $dt(CD)$ from all sources of 0.013 and 0.014 s for the two paths, respectively, using the method of Yang and Song (2020). Thus, the CD temporal changes are not significant within two standard deviations (95% confidence) and are well below the detection limit of 0.041 s by Yao et al. (2015) (their Table 2). The observed $ddt(SKp-CD)$ values also provide a direct reference, although the SKP has lower SNRs than PKP (CD or DF). The largest $ddt(SKp-CD)$ value is 0.031 s (Tables S3 and S4) and the estimated standard deviations are around 0.016 and 0.018 s following Yang and Song (2020) for the high-quality and inferior quality data sets, respectively. We didn't find any $ddt(SKp-CD)$ measurement that is significant at 95% confidence level. All of our error estimates didn't include possible influence of the preceding DF and coda energy on the CD phase as exemplified in Section 4. The influence would make the errors even larger but is hard to quantify. Incidentally, all the measurements are also about or below the de-

tection limits of Yao et al. (2015), suggesting that the method of using absolute times is not adequate to determine the CD temporal change even without considering clock errors.

5. Discussion and conclusion

5.1. Our preferred interpretation: changes from IC interior and differential IC rotation

We demonstrated above (in Section 4) that, at distances (128° to 142°) appropriate for the DF and CD phases, most (if not all) of the temporal changes are from the refracted DF phase rather than reflected CD phase. This suggests that the temporal changes are mainly from the interior of the IC rather than the ICB. The conclusion is also supported by previous existing observations. First, at larger distances ($>146^\circ$) when CD is absent, significant changes are observed in DF from BC-DF times (Fig. 1) along many ray paths (Song and Li, 2000; Zhang et al., 2005; Zhang et al., 2008; Yang and Song, 2020). The $ddt(BC-DF)$ can be over 0.3 s for the SSI-Alaska path (Zhang et al., 2005), several times larger than the largest $ddt(CD-DF)$. Globally, many data points of BC-DF temporal changes of over 0.05 s have been observed (Yang and Song, 2020) from high-quality doublets, while only two $ddt(CD-DF)$ are around 0.10 s from SSI doublets with less coherent waveforms and the rest are all smaller than 0.05 s. On the other hand, the reflected CD phase should be more sensitive to IC topographic changes than the transmitted DF phase. These observations are not consistent with temporal IC topographic changes. Furthermore, at even greater distances ($>155^\circ$), temporal changes in DF are either insignificant or much smaller (Li and Richards, 2003; Yang and Song, 2020). Temporal changes at the ICB would affect the DF phase at different distances similarly and thus these observations are again not consistent with temporal changes at the ICB. Second, temporal changes of IC scattering (ICS) waves of the pre-critical reflection PKiKP coda (at distances of 60 to 95°) have indicated differential IC rotation (Vidale et al., 2000; Vidale, 2019). The ICS waves are best explained by small-scale heterogeneity in the top part of the IC (Vidale et al., 2000; Leyton and Koper, 2007; Peng et al., 2008; Wu and Irving, 2017).

The above observations provide compelling evidence for internal changes in the upper part of the IC, rather than at the ICB. To explain the internal changes, a shift of the IC is the best and

simplest explanation so far. Furthermore, electromagnetic torque provides a ready mechanism for a differential IC rotation (Gubbins, 1981; Glatzmaier and Roberts, 1995). Thus, we still favor the interpretation of a differential rotation (Song and Richards, 1996; Zhang et al., 2005) for the observed IC temporal changes. In this interpretation, the temporal changes of the DF travel times are caused by a shift of the internal lateral velocity gradient of the IC (Creager, 1997) and the temporal changes of the ICS waves are caused by a shift of the internal small-scale heterogeneity of the IC (Vidale et al., 2000). Almost all the current non-zero estimates of the differential rotation rate are positive (faster rotation than the rotation of the Earth). In fact, a negative rotation rate can be ruled out (Song, 2000). This fact itself supports IC rotation as the probability of coincidence is very low.

5.2. Examination of contradictory observations and claims in previous studies

5.2.1. Claims of temporal changes solely from IC surface

In a series of papers, Wen (2006), Yao et al. (2015), and Yao et al. (2019) build a case that the observed IC temporal changes are solely from rapid and localized increase or decrease of the IC radius and they are not consistent with an IC rotation. Our conclusion is on the opposite side. Below we examine the key arguments in their studies.

Wen (2006) first observed temporal changes of the reflected CD phase using the 9303 doublet, discovered earlier by Zhang et al. (2005), and proposed two possible mechanisms at the ICB to explain the temporal changes, i.e., an IC rotation shifting ICB topography or a rapid localized IC growth. We examined exactly the same data (sampling Southern Africa) at Sections 4.1 and 4.3 and concluded that temporal changes occur mostly on DF arrivals while CD temporal changes cannot be reliably resolved. It appears that the mis-characterization by Wen (2006) was due to the intrinsic clock errors. By using SKP as a reference phase to form ddt measurements (rather than the absolute times from relocations), we were able to avoid the clock issue. Thus, the key observations of Wen (2006) or the foundation for the proposed ICB mechanisms can be rejected.

In a follow up paper, Yao et al. (2015) used 9 SSI doublets and found 5 of them have significant temporal changes in the absolute travel times of DF and/or CD phase after relocations. The paths with significant temporal changes are the same as Wen (2006) from SSI to stations AAK and ARU (sampling Southern Africa). They went a step further and attributed the changes (both in DF and CD) exclusively to localized increase or decrease of the IC radius. However, we believe their CD temporal changes are not reliable either. First, like Wen (2006), they also used absolute times (of both DF and CD phases) from relocations, which are subject to clock errors. Second, our new ddt measurements suggest the temporal changes are much larger in DF than in CD for the sampling region (Southern Africa). Including 9303 to AAK and ARU, we found a total of 16 ddt measurements with SKP reference phase, most (14) of which sample Southern Africa (open circles in Fig. 6, Table S4). The slopes suggest that more than 80% of the temporal changes in ddt(CD-DF) are from DF and less than 20% are from CD. Their data also give a clue – In their example waveforms (Fig. 1 of Yao et al., 2015), the DF phase shifts more than CD phase in most traces except the 9303 pair. Incidentally, our data quality is better than that in Yao et al. (2015). Because of insufficient SNRs, we excluded all four of their five doublets with temporal changes (at AAK or ARU) from our ddt measurements except the old 9303 doublet.

In a more recent follow up, Yao et al. (2019) further narrowed all IC temporal changes (including DF, DF coda, and CD) down solely to localized and rapid (even in days or months) changes of the IC surface and ruled out differential IC rotation. One key argu-

ment is that the rotation is not consistent with the behavior of the DF coda from the 9303 doublet to stations in Alaska and Canada. The argument is not convincing. First, the difference of the waveforms clearly starts from the DF onsets from many studies (e.g., Zhang et al., 2005) as well as their Fig. 2 and our Fig. 3 here. Second, the DF and coda waves along the path are very complex and energetic. The identifications of specific coda arrivals are difficult and the assumption of a single scatterer is questionable. The other arguments pertain to widely inconsistent estimates of the rotation rate from their data analyses, which we address below.

Yao et al. (2015) and Yao et al. (2019) also attributed temporal DF changes to the ICB. This is now contradictory to our result that there are little signals from the reflected CD phase. The observation of significant CD temporal changes is the crucial evidence that they attributed all the IC temporal changes to the ICB as a simple and consistent model because the CD phase is not affected by the IC interior.

In summary, the proposal of the ICB changes (Wen, 2006) as the sole source of the observed travel-time temporal changes (Yao et al., 2015; Yao et al., 2019) is not compatible with the following robust observations presented above. (1) The absolute travel times used in these studies are affected by random clock errors, which are impossible to be removed from relocations. The absolute-time based method cannot be used in the future for studies of temporal changes of less than 0.15 s (two standard deviations of the random clock errors; Yang and Song, 2020) unless the clock issue is resolved. (2) All of the temporal changes start at the onset of the DF phase. The later arriving CD phase could be affected by the time-varying DF phase and its coda, which is amply exemplified by the SSI-YKA data (Fig. 3). (3) For the paths which have much more coherent CD arrivals (which may indicate less influence from the DF and coda) as in the global data set, the CD temporal changes are not significant. (4) ICB temporal changes are not consistent with the distance-dependent temporal changes of the DF phase or the temporal changes of the ICS waves.

5.2.2. Claims of incompatible rotation rates

The large spread of the estimates of the differential rotation rate (see introduction) has been used to reject the IC rotation (Mäkinen and Deuss, 2011; Yao et al., 2019). Mäkinen and Deuss (2011) yield incompatible rates of a few tenths of a degree per year in both westward and eastward directions. Estimates by Yao et al. (2019) can vary by a factor of 27 along different paths. However, the argument is problematic for the following two reasons. First, measurement uncertainties need to be considered. Rotation rate estimates based on the DF travel time changes depend on the lateral velocity variations of underlying IC structure, which have large uncertainties, e.g., from mantle heterogeneities and fine-scale IC lateral variations. Recently, we found a new path from Chilean trench to Kazakhstan sampling North Atlantic that suggested a steep local ($\sim 2^\circ$) lateral velocity gradient of the IC and a slow eastward IC rotation of 0.05° per year (Yang and Song, 2020). The stations in Kazakhstan are far away from subduction zones and thus the gradient is less affected by mantle slab structure. On the other hand, the rate estimates based on the SSI-Alaska path, which provided early and most robust DF temporal changes, were $0.2\text{--}0.3^\circ$ per year or greater (e.g., Creager, 1997; Song, 2000; Zhang et al., 2005; Lindner et al., 2010). The sampled velocity gradient (beneath Central America) was measured across a much broader region over 25° in these studies, which is affected by slab structures beneath Alaska (Song, 2000; Frost et al., 2020). If the local velocity gradient is much greater than the smooth regional gradient, the estimated larger rotation rates for the SSI-Alaska path would be greatly reduced. For example, a 5 times increase of the local velocity gradient from the broad value would only need lateral difference of less than 0.2 s in differential BC-DF times over

a lateral distance of 2° , which would reduce the rotation rate to about $0.05\text{--}0.10^\circ$ per year from previous estimates. Confirmation and mapping of the local IC velocity gradients are important in future effort. Recently, Vidale (2019) derived a rotation of 0.07° per year between 1971 and 1974 based on the temporal shifts of strong blips of ICS waves, which does not require the precise knowledge of the underlying scatters. Thus it appears that all the observed temporal changes of seismic waves are best reconciled with a relatively slow rotation of around $0.05\text{--}0.1^\circ$ per year. Such a slow rotation is also consistent with a marginal rate from the normal-mode data (Laske and Masters, 2003). Second, there are not data that suggest the rotation rate must be constant at decadal time scale. In fact, there are suggestions that the IC rotation is not steady (Lindner et al., 2010; Tkalcic et al., 2013). However, those observations of non-steady rotation need to be carefully evaluated as they are inferred from the SSI to Alaska path, for which the IC structure is not well resolved to fine scales and is likely influenced by the slab effects (Frost et al., 2020).

Some extreme rotation rates have been reported (Waszak et al., 2011; Yao et al., 2019). Although it could represent a long-term average over the geological time, a rate of several degrees per million years (Waszak et al., 2011) would not result in any observable temporal changes of the seismic waves in current decades, thus can be easily rejected as the current rate of rotation. Yao et al. (2019) inferred a rate of at least 8.6° per year based on abrupt PKiKP temporal changes over 8–85 days and a rotation of IC topography. The inference is problematic due to the following. First, we have demonstrated above in the waveforms of DF and CD, the temporal changes may not come from CD (PKiKP). Second, their abrupt changes were not observed directly from doublets over days. They were inferred through a complicated process by using sequences of repeating earthquakes in close proximity. The temporal changes were initially observed from one sequence with lapses of a few years. The timing of the changes was narrowed down to only 8–85 days by removing the time spans without temporal changes from other sequences, assuming different sequences sampling the same IC structures. The assumption, however, is problematic, since the hypocenter differences between sequences are of a few tenths of degrees with uncertainties, which are comparable to IC fine-scale structures (Peng et al., 2008).

6. Conclusions

We examined systematically temporal changes of DF and CD waveforms using a large data set of repeating earthquakes (39 high-quality doublets, and 25 slightly inferior SSI doublets) and the non-IC SKP (or PP) reference phase. We found 23 SSI doublets recorded at YKA that have clear SKP (or PP) phase and 41 other doublet-station paths globally with clear SKP phase (thus PP phase is not needed). Except the SSI-YKA path, the DF and CD waveforms are highly similar (e.g., Figs. 2 and 4) and the differential times can be measured precisely (Fig. 6), which show ddt(CD-DF) values correlate much better with ddt(SKP-DF) than with ddt(SKP-CD). More than 80% of the temporal CD-DF changes come from the DF and no significant contributions from the CD are observed at 95% confidence. For the SSI-YKA path, the DF and coda waveforms change greatly (Fig. 3) and the CD arrivals are buried in the wave trains and hard to identify, making it not meaningful to measure the differential times. The differential waveforms show significant changes right from the DF onset and well before the predicted CD arrival time, suggesting that the CD arrivals can be contaminated by the time-varying DF and coda wave trains.

We conclude that the DF and CD temporal changes come mostly from the DF phase or the IC interior, rather than the CD phase or the ICB as in previous studies. Temporal changes of the ICB (Wen, 2006) as the sole source of the seismic wave changes (Yao et al.,

2015; Yao et al., 2019) can be ruled out. Our conclusion is consistent with temporal changes of the DF phase at larger distances and the ICS waves. The most probable and simplest explanation to the observed temporal changes is a differential rotation that shifts the position of the heterogeneous upper part of the IC. A rotation rate of about $0.05\text{--}0.1^\circ$ per year may reconcile all current temporal change observations from body waves, IC scattering, and normal mode data, but the rotation rate could vary even in decadal time scale.

Declaration of competing interest

The authors declare that they have no known competing financial interests or personal relationships that could be perceived as influencing the work reported in this paper.

Acknowledgements

We thank John Vidale and an anonymous reviewer for insightful and constructive comments, which help greatly improve the manuscript. The seismic data in this study were obtained from Incorporated Research Institutions for Seismology Data Management Center (<http://iris.edu>) and the Canadian National Seismograph Network (<http://earthquakescanada.nrcan.gc.ca/stndon/CNSN-RNSC/index-en.php>). Figures were plotted using GMT (Wessel and Smith, 1998). This research was supported by the National Science Foundation of the United States (EAR 1620595) and the National Natural Science Foundation of China (U1939204).

Appendix A. Supplementary material

Supplementary material related to this article can be found online at <https://doi.org/10.1016/j.epsl.2020.116267>.

References

- Cao, A., Masson, Y., Romanowicz, B., 2007. Short wavelength topography on the inner-core boundary. *Proc. Natl. Acad. Sci.* 104 (1), 31–35. <https://doi.org/10.1073/pnas.0609810104>.
- Cormier, V.F., Li, X., 2002. Frequency-dependent seismic attenuation in the inner core 2. A scattering and fabric interpretation. *J. Geophys. Res., Solid Earth* 107 (B12), ESE-14. <https://doi.org/10.1029/2002JB001796>.
- Creager, K.C., 1992. Anisotropy of the inner core from differential travel times of the phases PKP and PKIKP. *Nature* 356 (6367), 309–314. <https://doi.org/10.1038/356309a0>.
- Creager, K.C., 1997. Inner core rotation rate from small-scale heterogeneity and time-varying travel times. *Science* 278 (5341), 1284–1288. <https://doi.org/10.1126/science.278.5341.1284>.
- Fearn, D.R., Loper, D.E., Roberts, P.H., 1981. Structure of the Earth's inner core. *Nature* 292 (5820), 232–233. <https://doi.org/10.1038/292232a0>.
- Frost, D.A., Romanowicz, B., Roecker, S., 2020. Upper mantle slab under Alaska: contribution to anomalous core-phase observations on South-Sandwich to Alaska paths. *Phys. Earth Planet. Inter.* 299, 106427. <https://doi.org/10.1016/j.pepi.2020.106427>.
- Glatzmaier, G.A., Roberts, P.H., 1995. A three-dimensional convective dynamo solution with rotating and finitely conducting inner core and mantle. *Phys. Earth Planet. Inter.* 91 (1–3), 63–75. [https://doi.org/10.1016/0031-9201\(95\)03049-3](https://doi.org/10.1016/0031-9201(95)03049-3).
- Gubbins, D., 1981. Rotation of the inner core. *J. Geophys. Res.* 86 (B12), 11695–11699. <https://doi.org/10.1029/JB086iB12p11695>.
- Kennett, B.L.N., Engdahl, E.R., 1991. Traveltimes for global earthquake location and phase identification. *Geophys. J. Int.* 105 (2), 429–465. <https://doi.org/10.1111/j.1365-246X.1991.tb06724.x>.
- Laske, G., Masters, T.G., 2003. The Earth's free oscillations and the differential rotation of the inner core. In: Veronique Dehant, K.C.C., Karato, S.-I., Zatman, S. (Eds.), *Earth's Core: Dynamics, Structure, Rotation*. Washington, DC: American Geophysical Union. In: AGU Dynamics Series, vol. 31, pp. 5–21 (Chap. 1). <https://doi.org/10.1029/GD031p0005>.
- Leyton, F., Koper, K.D., 2007. Using PKiKP coda to determine inner core structure: 1. Synthesis of coda envelopes using single-scattering theories. *J. Geophys. Res., Solid Earth* 112 (5), 1–19. <https://doi.org/10.1029/2006JB004369>.
- Li, A., Richards, P.G., 2003. Using earthquake doublets to study inner core rotation and seismicity catalog precision. *Geochem. Geophys. Geosyst.* 4 (9). <https://doi.org/10.1029/2002GC000379>.

- Lindner, D., Song, X., Ma, P., Christensen, D.H., 2010. Inner core rotation and its variability from nonparametric modeling. *J. Geophys. Res.* 115, B04307. <https://doi.org/10.1029/2009JB006294>.
- Mäkinen, A.M., Deuss, A., 2011. Global seismic body-wave observations of temporal variations in the Earth's inner core, and implications for its differential rotation. *Geophys. J. Int.* 187 (1), 355–370. <https://doi.org/10.1111/j.1365-246X.2011.05146.x>.
- Peng, Z., Koper, K.D., Vidale, J.E., Leyton, F., Shearer, P., 2008. Inner-core fine-scale structure from scattered waves recorded by LASA. *J. Geophys. Res., Solid Earth* 113 (9), 1–11. <https://doi.org/10.1029/2007JB005412>.
- Poupinet, G., Ellsworth, W.L., Frechet, J., 1984. Monitoring velocity variations in the crust using earthquake doublets: an application to the Calaveras Fault, California. *J. Geophys. Res., Solid Earth* 89 (B7), 5719–5731. <https://doi.org/10.1029/JB089iB07p05719>.
- Poupinet, G., Souriau, A., Coutant, O., 2000. The existence of an inner core super-rotation questioned by teleseismic doublets. *Phys. Earth Planet. Inter.* 118 (1–2), 77–88. [https://doi.org/10.1016/S0031-9201\(99\)00129-6](https://doi.org/10.1016/S0031-9201(99)00129-6).
- Song, X., 2000. Joint inversion for inner core rotation, inner core anisotropy, and mantle heterogeneity. *J. Geophys. Res., Solid Earth* 105 (B4), 7931–7943. <https://doi.org/10.1029/1999jb000436>.
- Song, X., 2001. Comment on "The existence of an inner core super-rotation questioned by teleseismic doublets" by Georges Poupinet, Annie Souriau, and Olivier Coutant. *Phys. Earth Planet. Inter.* 124 (3–4), 269–273. [https://doi.org/10.1016/S0031-9201\(01\)00182-0](https://doi.org/10.1016/S0031-9201(01)00182-0).
- Song, X., Dai, W., 2008. Topography of Earth's inner core boundary from high-quality waveform doublets. *Geophys. J. Int.* 175 (1), 386–399. <https://doi.org/10.1111/j.1365-246X.2008.03909.x>.
- Song, X., Helmberger, D.V., 1993. Anisotropy of Earth's inner core. *Geophys. Res. Lett.* 20 (23), 2591–2594. <https://doi.org/10.1029/93GL02812>.
- Song, X., Li, A., 2000. Support for differential inner core superrotation from earthquakes in Alaska recorded at South Pole station. *J. Geophys. Res., Solid Earth* 105 (B1), 623–630. <https://doi.org/10.1029/1999JB000341>.
- Song, X., Richards, P.G., 1996. Seismological evidence for differential rotation of the Earth's inner core. *Nature* 382 (6588), 221–224. <https://doi.org/10.1038/382221a0>.
- Song, X., Xu, X., 2002. Inner core transition zone and anomalous PKP (DF) waveforms from polar paths. *Geophys. Res. Lett.* 29 (4), 1. <https://doi.org/10.1029/2001GL013822>.
- Souriau, A., Roudil, P., Moynot, B., 1997. Inner core differential rotation: facts and artefacts. *Geophys. Res. Lett.* 24 (16), 2103–2106. <https://doi.org/10.1029/97GL01933>.
- Sun, X., Poupinet, G., Song, X., 2006. Examination of systematic mislocation of South Sandwich Islands earthquakes using station pairs: implications for inner core rotation. *J. Geophys. Res., Solid Earth* 111, B11305. <https://doi.org/10.1029/2005JB004175>.
- Tkalčić, H., Young, M., Bodin, T., Ngo, S., Cambridge, M., 2013. The shuffling rotation of the Earth's inner core revealed by earthquake doublets. *Nat. Geosci.* 6 (6), 497–502. <https://doi.org/10.1038/ngeo1813>.
- Vidale, J.E., 2019. Very slow rotation of Earth's inner core from 1971 to 1974. *Geophys. Res. Lett.* 46 (16), 9483–9488. <https://doi.org/10.1029/2019GL083774>.
- Vidale, J.E., Dodge, D.A., Earle, P.S., 2000. Slow differential rotation of the Earth's inner core indicated by temporal changes in scattering. *Nature* 405 (6785), 445–448. <https://doi.org/10.1038/35013039>.
- Waszek, L., Irving, J., Deuss, A., 2011. Reconciling the hemispherical structure of Earth's inner core with its super-rotation. *Nat. Geosci.* 4 (4), 264–267. <https://doi.org/10.1038/ngeo1083>.
- Wen, L., 2006. Localized temporal change of the Earth's inner core boundary. *Science* 314 (5801), 967–970. <https://doi.org/10.1126/science.1131692>.
- Wessel, P., Smith, W.H.F., 1998. New, improved version of generic mapping tools released. *Eos Trans. AGU* 79 (47), 579. <https://doi.org/10.1029/98EO00426>.
- Wu, W., Irving, J.C.E., 2017. Using PKiKP coda to study heterogeneity in the top layer of the inner core's western hemisphere. *Geophys. J. Int.* 209 (2), 672–687. <https://doi.org/10.1093/gji/ggx047>.
- Xin, D., Song, X., Wang, T., 2015. Localized temporal variation of Earth's inner-core boundary from high-quality waveform doublets. *Earth Sci.* 28 (3), 175–185. <https://doi.org/10.1007/s11589-015-0125-0>.
- Yang, Y., Song, X., 2020. Temporal changes of the inner core from globally distributed repeating earthquakes. *J. Geophys. Res., Solid Earth*, e2019JB018652. <https://doi.org/10.1029/2019JB018652>.
- Yao, J., Sun, L., Wen, L., 2015. Two decades of temporal change of Earth's inner core boundary. *J. Geophys. Res., Solid Earth* 120 (9), 6263–6283. <https://doi.org/10.1002/2015JB012339>.
- Yao, J., Tian, D., Sun, L., Wen, L., 2019. Temporal change of seismic Earth's inner core phases: inner core differential rotation or temporal change of inner core surface? *J. Geophys. Res., Solid Earth* 124 (7), 6720–6736. <https://doi.org/10.1029/2019JB017532>.
- Zhang, J., Richards, P.G., Schaff, D.P., 2008. Wide-scale detection of earthquake waveform doublets and further evidence for inner core super-rotation. *Geophys. J. Int.* 174 (3), 993–1006. <https://doi.org/10.1111/j.1365-246X.2008.03856.x>.
- Zhang, J., Song, X., Li, Y., Richards, P.G., 2005. Inner core differential motion confirmed by earthquake waveform doublets. *Science* 309 (5739), 1357–1360. <https://doi.org/10.1126/science.1113193>.